The 2017 World Congress on
Advances in Structural Engineering and Mechanics (ASEM17)
28 August - 1 September, 2017, Ilsan(Seoul), Korea

Influence of staggered position of a square cylinder of different height on the wake of downstream square cylinder near a plan wall

*Rajesh Bhatt[1)], Dilip K. Maiti[2)] and Md. Mahbub Alam[3)#]

[1&3)] *Institute for Turbulence-Noise-Vibration Interaction and Control, Shenzhen Graduate School, Harbin Institute of Technology, Shenzhen, China*
[2)] *Department of Applied Mathematics with Oceanology and Computer Programming, Vidyasagar University, Midnapur 721102, India*
[#]*alamm28@yahoo.com*

ABSTRACT

A numerical study is conducted on two-dimensional flow over two staggered cylinders at a Reynolds number of 100. The governing equations are solved numerically through a pressure-correction-based iterative algorithm (SIMPLE) with the quadratic upwind interpolation for convective kinematics (QUICK) scheme for convective terms. The incident flow is a linear shear flow. The downstream cylinder is square, of height A, positioned near a wall with a gap height of 0.5A. The upstream cylinder is also square, but of different sizes, with height ratio $a^* = a/A$ = 1 and 0.5, respectively. In order to investigate the effect of position and a^* of the upstream cylinder on the flow around and aerodynamic forces acting on the downstream cylinder, the gap height between the wall and upstream cylinder L^*(= L/A = 0.1-3.0) and the streamwise spacing between the cylinders S^*(=S/A= 0.5-7.0) are varied systematically. The flow structure around the downstream cylinder is highly dependent on L^* and a^*, experiencing several discontinuities. For the same L^*, the interaction between vortices from the two cylinders is weaker for a^* = 0.5 than for a^* = 1.0, as such very small peaks are observed in the spectra of the lift coefficient of downstream cylinder for a^* = 0.5.

NOMENCLATURE

a :height of the upstream square cylinder (m)
A :height of the downstream square cylinder (m)
L^* :nondimensional gap height from upstream cylinder to plane wall
S^* :nondimensional gap spacing between the cylinders
Re :Reynolds number (UA/v)
C_D :normalized time averaged drag coefficient
C_L :normalized time averaged lift coefficient
C_L' :rms of lift coefficient
St :Strouhal number
U :velocity at height A from the wall (m/s)
V : kinematic viscosity of fluid
$\overline{C_P}$: time averaged pressure coefficient

1. INTRODUCTION

Flow past cylinders is found in many practical engineering applications such as, compact heat exchangers, cooling of electronic components, drying of different materials (textiles, veneer, paper and film materials), cooling of glass, plastics and industrial devices, and so on. In order to accurately design the devices and structures, forces and interference effect of the neighbouring structures should be well understood. Both position and shape of neighbouring structure affect the flow pattern around a structure. For two tandem cylinders, the downstream cylinder is submerged in the wake of the upstream one. However, when the upstream cylinder is offset with respect to the downstream cylinder, vortex shedding mechanism and the force characteristics differ significantly from the inline case. There is a significant volume of articles on the flow around a single and tandem square cylinders. To our knowledge, there is no article available on the flow around a square cylinder in presence of the upstream cylinder of different heights. In the present study, square cylinders are chosen because they can easily be given a Cartesian grid system with higher accuracy. This study is important for many applications mentioned above, providing also some fundamental information of the flow around cylinders in the staggered arrangement.

Studies on the problems of wake development and vortex shedding behind a rectangular cylinder in free-stream flows were investigated both numerically and experimentally by Davis and Moore (1982), Franke et al. (1990) and Okajima et al. (1990). When the cylinder is placed in the proximity of a solid wall, the strength of the upper and lower shear layers separated from the surfaces of the cylinder is not identical and the vortex shedding pattern is therefore distorted. The effect of wall proximity on the flow around a single cylinder was investigated by Martinuzzi et al. (2003), Bhattacharyya and Maiti (2004), Mahir (2009), Harichandan and Roy (2012) and Maiti (2012). Bhattacharyya and Maiti (2004) observed that the vortex shedding frequency from a square cylinder near a wall is higher for a shear flow than the uniform flow. The dependence of flow characteristics of a rectangular cylinder near a wall on the incident shear flow velocity and gap height has been reported in the previous studies (Maiti, 2011, 2012).

The flow around two staggered circular cylinders has been extensively studied experimentally (Sumner (2000), Alam et al. (2005), Zhou et al. (2009)) and numerically (Lee et al. (2009), Akbari and Price (2005)). Nine flow patterns are identified, and processes of shear layer reattachment, induced separation, vortex pairing and synchronization, and vortex impingement, are elucidated by Sumner (2000). Akbari and Price (2005) identified five flow patterns, depending on the geometrical arrangement of the cylinders at a subcritical Reynolds number (Re) of 800. Lee et al. (2009) numerically identified ten distinct flow patterns for two circular cylinders at $Re \leq 160$. Alam et al. (2017) investigated flow around four side-by-side circular cylinders at $Re = 100$. They identified four flow regimes (single bluff-body, flip-flopping, quasi-interlocked, and interlocked flow) depending on the gap spacing between the cylinders.

Balachandar and Parker (2002) considered the onset of vortex shedding in a periodic array of rectangular cylinders in both inline and staggered arrangement. They observed that the interaction between the cylinders becomes negligible when the transverse spacing between the cylinders is large enough and the critical *Re* approaches that of an isolated cylinder. Niu and Zhu (2006) in a numerical study of three-dimensional flow around two identical square cylinder in staggered arrangements evaluated the dependence of aerodynamic characteristics on the streamwise spacing. Sewatkar et al. (2009) performed a numerical study of the flow around a row of nine square cylinders placed normal to the oncoming flow. They identified different flow regimes based on the gap spacing of cylinders and proposed that wake interaction is strongly influenced by the jets in the gap region. Chatterjee et al. (2010) performed a numerical study for the flow around five square cylinders placed side-by-side and normal to the oncoming flow at *Re* = 150. Burattini and Agarwal (2013) with change in spacing between two side-by-side square cylinders observed various flow structures. Chern et al. (2010) observed a jet-like structure when oscillatory flows are given through the gap of two side-by-side cylinders.

Rosales et al. (2001) compared results of the inline and offset square cylinder pairs at a fixed spacing ratio of 2. Their study revealed pronounced differences in the unsteady flow behaviour between the inline and offset pairs. Devarakonda (1994) examined the case of offset square cylinders exposed to a uniform flow at a fixed spacing ratio of 3 and observed that the Strouhal number is larger than that for an inline cylinders. Malekzadeh and Sohankar (2012) reported three major flow regimes depending on the height and position of a control plate upstream of a square cylinder. Bao et al. (2012) showed six different flow patterns, which appeared successively with the increase of spacing between six inline square cylinders. For a pair of inline square cylinders, Bhattacharyya and Dhinakaran (2008) observed that the onset of vortex shedding occurs for *Re* beyond 125 for all spacing (0.5- 5) examined. Maiti and Bhatt (2014a, 2014b) extended the above study considering the upstream cylinder as rectangular shape of different heights and widths in a tandem arrangement. It is reported that the transition (-from unsteady/steady to steady/unsteady-) of the flow over the upstream/downstream cylinder strongly depends on the shape and the position of the upstream cylinder.

The above literature review indicates that shedding frequencies, aerodynamic forces and wakes of two or a group of cylinders are dependent on the inter-cylinder spacing, flow incidence angle and the cylinder shape. Although there are a number of studies on single cylinder and pair of cylinders, the flow past a square cylinder in presence of another square cylinder in staggered or tandem arrangement has not received much attention, especially for the case of incident shear flow. Here the objective of the work is to examine the wake flow structure, aerodynamic forces, and shedding frequency of a square cylinder lying in the wake an upstream square cylinder where the height and position of the upstream cylinder are varied. The effect of inter-cylinder spacing, shape of upstream cylinder, and gap height of upstream cylinder from a plan wall on the flow characteristics of the downstream square cylinder are investigated for uniform shear flow. Simulations have been performed for two different heights of the upstream

cylinder a*=1.0 and 0.5 at fixed Reynolds number of 100. By keeping the position of the downstream cylinder fixed, the range of S^* and L^* are chosen as $0.5 \le S^* \le 7.0$ and $0.1 \le L^* \le 3.0$.

2. PROBLEM FORMULATION

A wall lying along the x-axis and a long cylinder of square cross-section of height A is placed parallel to the wall at a fixed gap height $0.5A$ from the wall, as below this height suppression of vortex shedding for $Re<125$ was reported in the previous study (Bhattacharyya and Maiti, 2004). Another cylinder of square cross-section of height ratio $a^*(=a/A)$ - with height a is placed at a distance $S^*(=S/A)$ from the upstream face of the square cylinder and parallel to the wall at different gap ratios $L^*(=L/A)$ from the wall (see Fig. 1). The upstream flow field is taken as uniform shear flow based velocity profile $u^*(y^*)$. This upstream condition is consistent with the Navier-Stokes equation and viscous effects. In other words, the cylinders are submerged into the boundary layer of a plane wall. The upstream flow field is taken as a uniform shear flow $u^* = Uy^*/A$ with no pressure gradient where U is the velocity at height A from the wall. As there is no velocity scale U directly, the prescribed slope λ of the incident velocity profile at the surface multiplied by A, leaving $U = \lambda A$ is taken as the velocity scale. It may be noted that there will not be any incidence flow if the velocity gradient λ approaches zero. The Reynolds number can be defined as $Re=UA/v$, where v is kinematic viscosity.

The governing equations for two-dimensional laminar flow are as follows:

$$\nabla \cdot V = 0 \tag{1}$$

$$\frac{\partial V}{\partial t} + (V \cdot \nabla)V = -\nabla p + \frac{1}{\mathrm{Re}}\nabla^2 V \tag{2}$$

where $V=(u, v)$, and p and t denote the velocity, pressure and time, respectively. All the variables are nondimensionalized by A and U.

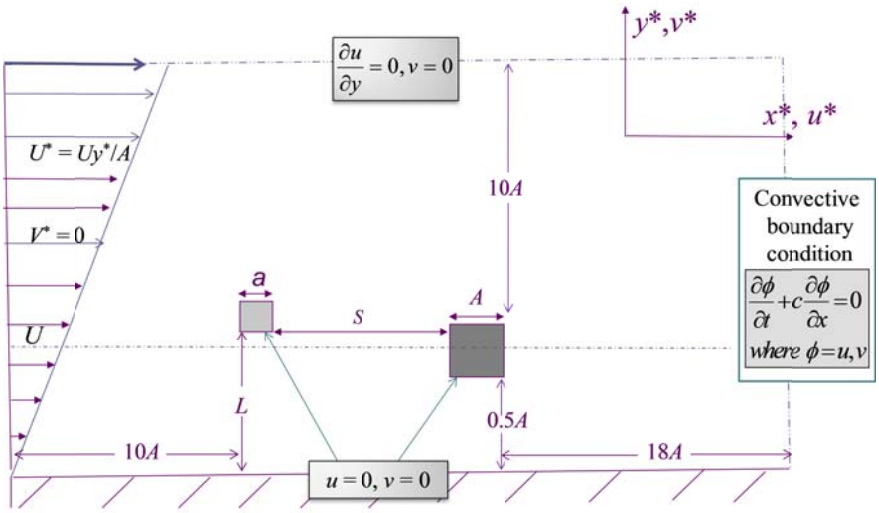

Fig.1. Schematics of the flow configuration.

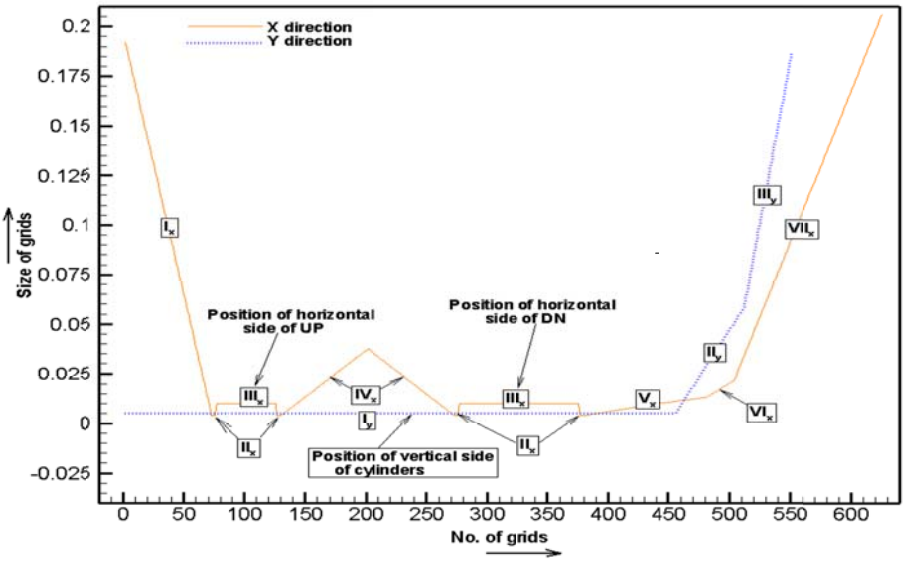

Fig. 2. The control volume size distribution along x *and y*-direction for *a**=0.5 and *S**=3.0 for *L**=1.5.

3. BOUNDARY CONDITIONS AND NUMEICAL METHOD

The height of the top lateral boundary and inflow boundary are chosen large enough so that the influence of the boundary conditions on the wall shear stress is very weak. The inflow and outlet boundaries lies at a distance X_{inlet} = 10*A* and X_{outlet} = 18*A* from the front face of the upstream cylinder and rear face of the downstream cylinder, respectively. While the top lateral boundary lies at Y_{top} = 10*A* from the top face of the upstream cylinder. A non-uniform grid distribution is considered distributing uniform grids along the surfaces of both the cylinders with expansion factors for the far-fields (away from the surfaces) starting with δ1. The grids distribution in x- and y- directions is shown in Fig. 2 for the arrangement with *a**=0.5, *S** = 3 and *L** = 1.5. Depending on the size of distributed grids, the horizontal and vertical lines of the computational domain can be divided into seven and three, respectively, distinct segments. A symmetry grid (along the x-direction about the mid-line in the spacing between the cylinders) starting with δ1 from any one of the interfacing face is incorporated (segment-IV_x in Fig. 2). Along the y-direction, a uniform grid with size δ1=0.005 is considered between wall and top of the upstream cylinder (within the segment I_y in Fig. 2). The grid refinement study on the number of uniform nodes and on the resolution of grid sizes in the spacing distance and the far-fields was conducted in our previous study (Maiti and Bhatt (2014a)) for inline tandem cylinders is used in the present study. In the case of *a**=0.5, *S** = 3.0, *L**=1.5 (Fig. 2), for instance, the total number of control volumes were 625 × 550, with the first and the second number being the number of mesh points in the x and y-direction, respectively. For other combination, the number of grid points are used by increasing/decreasing the number of grid distributed in the spacing distance only. The gird along y-direction is dependent on the value of *a** and *L**.

A Dirichlet boundary ($u=u(y)$, $v=0$) is used at the inlet boundary, while the convective boundary condition (Maiti, 2011) $(\partial\phi/\partial t)+u_c(\partial\phi/\partial x)=0$, where ϕ is any flow variable, and

u_c is the local wave speed) is applied at the outlet. No-slip condition is used on the cylinders surfaces and on the plane wall. A slip boundary condition ($\partial u/\partial y$=0, v=0) is imposed on the top lateral boundary.

The computational domain is divided into Cartesian cells. A finite volume method (FVM) on a staggered grid system is used to solve the governing equations. The discretized equations are than solved by the pressure correction based iterative algorithm SIMPLE (Patankar (1980)), are applied. A third order accurate Quadratic Upwind Interpolation for Convective Kinematics (QUICK) (Leonard (1995)) is employed to discretize the convective terms and central differencing scheme for diffusion terms. A fully implicit second order scheme is incorporated to discretize the time derivatives. At the initial stage of motion, Δt is taken to be 0.0001 which has been subsequently increased to 0.001 after the transient state. A detailed discussion of the numerical methodology (staggered grid, FVM, QUICK and SIMPLE algorithms) used here has been made in the previous study (Bhattacharyya et al. (2006)).

4. VALIDATION OF NUMERICAL CODE

In order to verify the numerical code and grid resolution, simulations were conducted in the previous studies Maiti (2011, 2012) for single cylinder and Maiti and Bhatt (2014, 2015) for tandem cylinders has been used in the present study. This code was validated for the case of (i) a square cylinder without plane wall for different *Re* (Bhattacharyya and Maiti (2005)), (ii) a square cylinder placed in a boundary layer at a gap height from a wall (Bhattacharyya et al. (2006)) and (iii) a square cylinder confined in a channel (Bhattacharyya and Maiti (2004)). The numerical methodology used in the present study is same as used in our previous study on tandem cylinders (Maiti and Bhatt (2014a, 2014b)). The detail discussion has been made in our previous study (Maiti and Bhatt, (2014a) : ref. Fig. 2 and 3, and Table-2). The grid independent results and comparison reveal a satisfactory agreement and would, hence, boost confidence in the generated results, which are believed to be good enough for showing up correct influence of physical parameters.

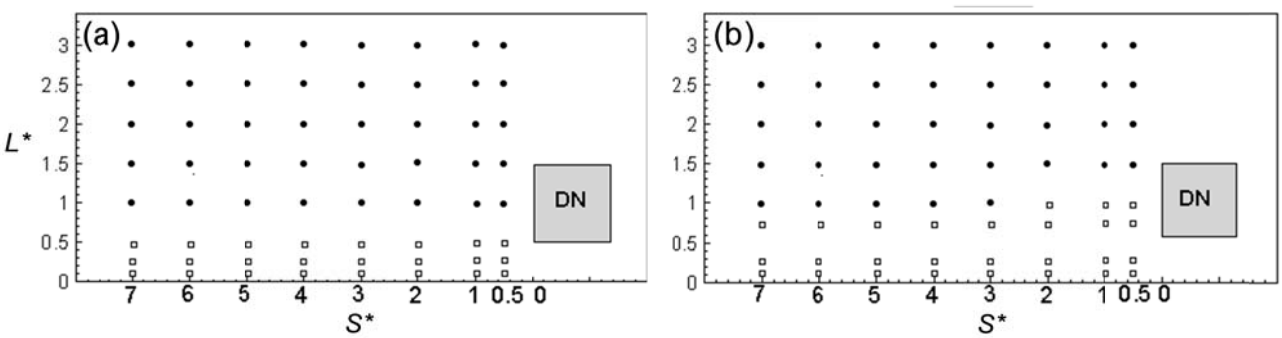

Fig. 3. Location of the upstream square cylinder with respect to the downstream square cylinder and wall. (a) a^*=1.0 and (b) a^*=0.5. Solid dots : unsteady flow, Blank dots : steady flow.

5. RESULTS AND DISCUSSION

5.1 Flow structure

The simulations are performed for different *a** and different locations (*L**, *S**) of the upstream cylinder with respect to the downstream square cylinder and wall (see Fig. 3). The dots indicate the cases of actual computations.

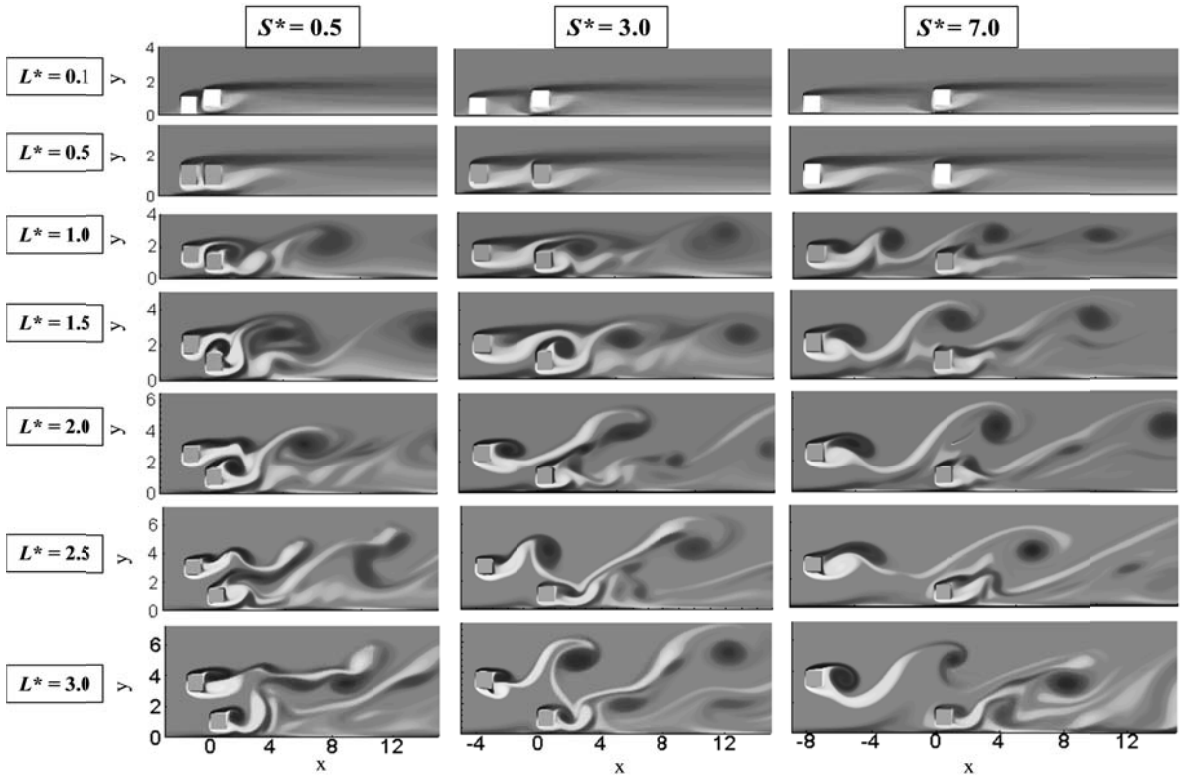

Fig. 4. Instantaneous vorticity contours for *a**=1.0 at different *L** and *S**.

In the previous study for shear flow past a single square cylinder in wall proximity (*L** = 0.5), Bhattacharyya and Maiti (2004) found that the wake remains steady up to Reynolds number 125. Maiti and Bhatt (2014, 2015) reported that the unsteadiness in the steady flow of the downstream cylinder at Re < 125 can be generated employing an upstream cylinder of rectangular shape against the approaching flow to the downstream cylinder after certain spacing *S** (=S_{cr}). It was also observed that for two cylinders in tandem, the critical spacing ratio is sensitive to the Reynolds number, height and width of the upstream cylinder. In the present study, series of flow visualization are produced from the simulations, which are used to study the flow behavior for different configurations of the staggered pair of cylinders. At lower *L**, particularly for closely spaced configuration the cylinders are situated very close to one another and the gap between the cylinders is small. The wake region of upstream is narrow as it is constrained by the gap height and the inter cylinder distance. The shear layers from the upstream cylinder remains attached with the downstream cylinder and flow remains steady from the downstream cylinder. At lower gap height under the

uniform shear flow the flow field is similar to a single bluff body flow. For the inline tandem arrangement the flow remains steady from both the cylinders and the recirculation length behind the downstream cylinder is increased.

With the increase of gap height ($L^* \approx 1.0$) for lower S^*, the shear layers either wraps around or reattaches on the downstream cylinder. The positive shear layers from the upstream cylinder are enveloped by the negative shear layer of both the cylinders and then forced the negative shear layers pf the downstream cylinder interact with positive counterpart. If one compares the formation of vortices from the cylinders with the larger S^*, it is clearly perceived that the upstream cylinder vortices shed in the gap between the cylinders. Further increase in L^* results small positive vortices from the wake of the downstream cylinder for intermediate spacing. When the cylinder is located in the higher velocity zone a wider wake is formed behind the cylinder. The negative vortices from the upstream cylinder has less impact on the shear layers of the downstream cylinder. However, the positive vortices from the upstream cylinder hit the downstream cylinder and then roll. As results, the positive vortices are stretched towards the wake of the cylinder. The strength of the negative shear layers around the downstream cylinder is effectively reduces. The negative vortices found in the wake are mainly from the upstream cylinder.

For $L^* \geq 2$, the vortices shed from the upstream cylinder evolves in the vertical direction. Higher the gap height of upstream cylinder from the wall, the more elongation of the positive shear layers from the upstream cylinder towards downstream. The shear layers do not roll-up completely and the effect of the vortices on the downstream cylinder reduces. The vortices behind the downstream cylinder are fairly close to each other. They interact with each other, forming a very complex wake. Such vortex interaction results in more complex wake interference around the downstream cylinder. The vortex shed from the upstream cylinder attacks the front face of the downstream cylinder at lower L^*. However, at higher L^* instead of impinging on the front face, vortices pass through the upper surface of the downstream cylinder.

Fig. 5 shows the effect of reduction of height of the upstream cylinder on flow structure for different S^* and L^*. The effect of decreasing the height of the upstream cylinder is clearly visible from the vorticity contours. The flow pattern for the case of $a^*=1.0$ is more complex in comparison to the case of $a^*=0.5$. The positive and negative vortices shed alternately from the upstream cylinder and consequently move downstream. It is noticed that with reduction in height the elongated vortices are reduced. With the increase of L^*, the positive vortices are more elongated and dominate the wake. The negative vortices from the upstream cylinder are fairly round whereas positive vortices being oblate in shape. With the increase in L^* the interaction between the vortices decreases. The wake flow of the upstream cylinder of square shape is similar to the wake of a single square cylinder under the shear flow (Saha et al. (2003) and Cheng et al. (2005)).

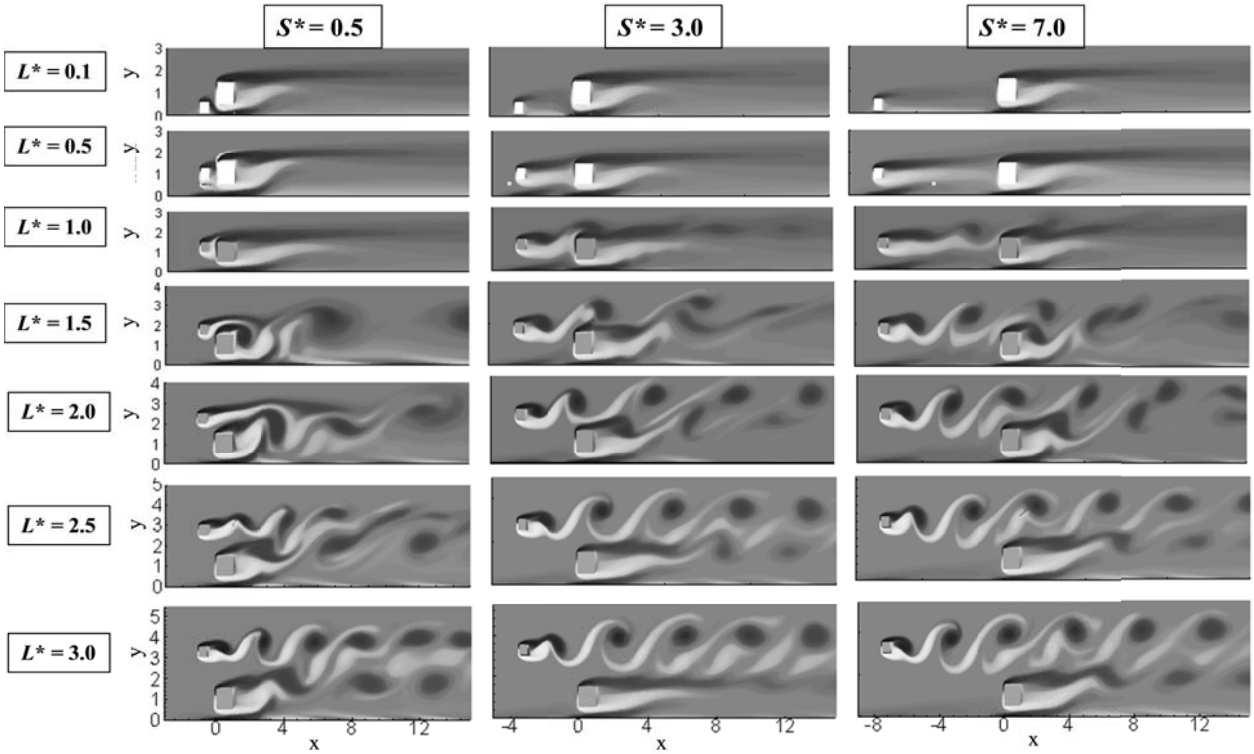

Fig. 5. Instantaneous vorticity contours for a^*=0.5 at different L^* and S^*.

As it can be seen from Fig. 4 and 5 that unsteady flow is observed for both a* by offsetting the upstream cylinder from its inline position. The offsetting of the upstream cylinder from the wall is equivalent to expose the upstream cylinder in the higher velocity zone. For the staggered position of cylinder, the strength and direction of the gap flow vary with the height of the upstream cylinder, either deflected towards the cylinder or directed along the centerline. As plotted in Fig. 4 and 5, the critical spacing is dependent on the height of the upstream cylinder and its gap height from wall, also mathematically, $S_{cr} = S_{cr}(a^*, L^*)$. The value of critical spacing S_{cr} is increased by reducing the height of the upstream cylinder.

From the ongoing discussion it is clear that the unsteadiness in the steady flow of a square downstream cylinder can be generated at a particular gap height L^* by offsetting the upstream cylinder at a Re < 125. At the same time, one can deduce from the discussion based on Fig. 4 and Fig. 5 that the dynamic interaction between the vortices shed from the upstream cylinder and the shear layers separated from the leading edge of the downstream cylinder reduces with the increase of gap height after certain gap height L^*. As a consequence, the original steady/unsteady flow of an isolated square cylinder is to be expected from the downstream cylinder in the physical domain after a certain large L^* (say, L_{cr} : the upper bound for L_{cr}). Beyond this L_{cr} there should not be any effect on the behavior of flow over the downstream cylinder due to the presence of the upstream cylinder. Consequently, the following inequality for $L_{cr}(a^*, S^*)$ can be established : $L_{cr}(1.0, S^*) > L_{cr}(0.5, S^*)$.

5.2 Shedding frequency and fluctuating forces

In order to delineate the effect of presence of the upstream cylinder of different heights at different S^* and L^* on amplitude of fluctuation of the forces on the downstream cylinder, the spectra of lift coefficient of the downstream cylinder is presented in Fig. 6 for S^*=0.5, 3.0 and 7. Each figure shows the effect of gap height of the upstream cylinder from the wall on amplitude of fluctuating lift coefficient for a particular combination of S^* and L^*. Examining the individual spectra (Fig. 6), there is variation in the shape and strength of the vortex shedding peak with change in L^*. At lower S^* (≈ 0.5), the intensity of the peak of power spectra decreases with the increase in L^* particularly for a^*=0.5. For the upstream cylinder near wall the weaker peaks are observed in the spectra of the downstream cylinder. The peak becomes stronger with increase in L^* for a particular S^*(≥ 3). Among all the multiple peaks the dominant peak indicates the Strouhal number corresponding to the main shedding frequency of the primary Karman vortices and the secondary frequency of the downstream cylinder can therefore be regarded as cylinder interference frequency. While for a^*=0.5 the interaction of vortices of both cylinders decreases with the increase in L^* and very small peaks are observed in the spectra of the downstream cylinder at large L^*. It is expected that the upstream cylinder do not have a significant effect on the vortex shedding of the downstream cylinder at large gap height.

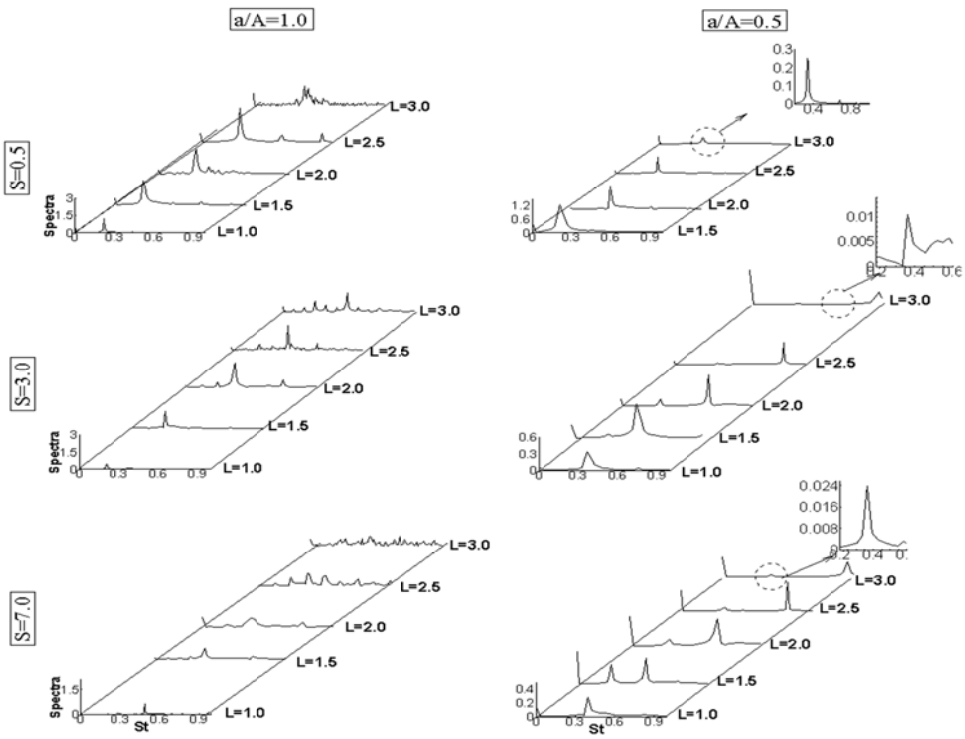

Fig. 6. Spectra of lift coefficient of downstream cylinder for different L^* and S^*.

The vortex shedding frequency is analyzed based on the values of the Strouhal number (St) calculated at the dominant peak in the spectra of lift coefficient (C_L) of the

downstream cylinder. Figure 7 shows contour plots for the variation in *St* of the downstream cylinder with gap height (*L**) for each *a** at different spacing *S**. The variation in *St* at both *a** showed qualitatively similar behavior with changein *L**. There is some degree of scatter in the *St* when *L** varies. As it is observed in Fig. 6 the vortex shedding peak are small at lower *L**. The shedding frequency of the downstream cylinder increases with the increase in *L** as well as with the decrease *a**. At this *Re* = 100 (when the flow of an isolated square cylinder is steady), the wake oscillation frequency for the flow past a square cylinder in presence of an upstream cylinder is completely overwhelmed by that of the respective upstream cylinder. Apparently, the same *St* for both the cylinders is observed here. The increment in the *St* due to *L** may be attributed to the fact that the upstream cylinder is exposed to a higher velocity region when it is moved far from the wall. It is reported in Maiti (2011) for an isolated cylinder that the *St* at *Re* = 50 is more than that at *Re* = 100. Therefore, the increment in *St* due to reduction in height of the upstream cylinder at *Re* = 100 may be due to reduction in the local Reynolds number. However, due to reduced interference of vortices, the low *St* persists with further increase in *L**.

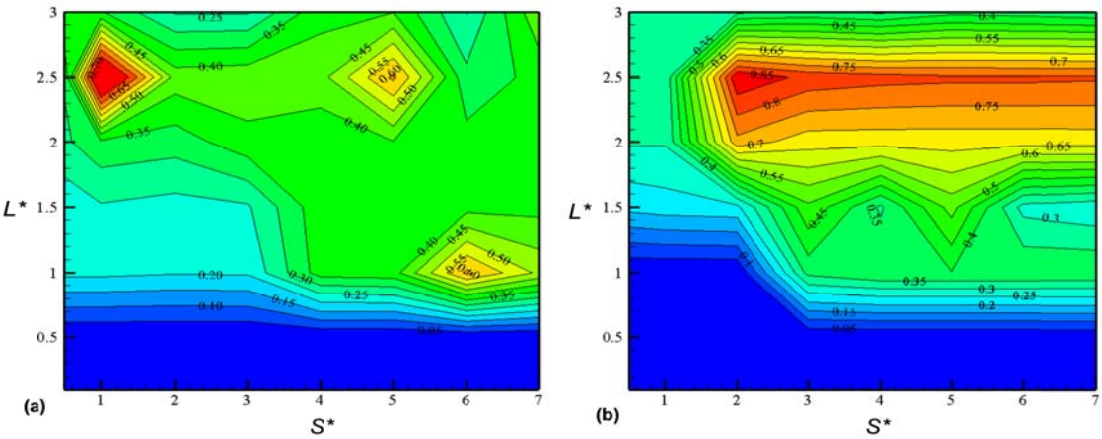

Fig. 7. Contours of vortex shedding frequency (*St*) of the downstream cylinder (a) *a**=1.0 and (b) *a**=0.5 at different *L** and *S**.

The magnitude of the fluctuating lift can be represented by the root-mean-square (RMS) value: C_L'. The results of C_L' of the downstream cylinder against *L** at different *S** are summarized in the contour plots in Fig. 8 for different *a**. Inspection of the figures discloses the fact that the C_L' of the downstream cylinder increases with increase in *L** reaching their respective maximum value and then started to decrease for further increase in *L** to reach zero value, the case of steady flow of the downstream cylinder for *a**= 1.0. This increment is because the flow interaction of the upstream cylinder with the downstream cylinder causes to amplify the fluctuations of forces of the downstream cylinder. The enhancement in the amplitude of fluctuating forces of the downstream cylinder is more at the intermediate spacing (*S** = 3). The reduction of height of the upstream cylinder results reduction in RMS value of the downstream cylinder for all *S**. Beyond *L** = 2.0, the effect of the upstream cylinder of *a**= 0.5 on the fluctuation of the lift coefficient of the downstream cylinder is almost negligible.

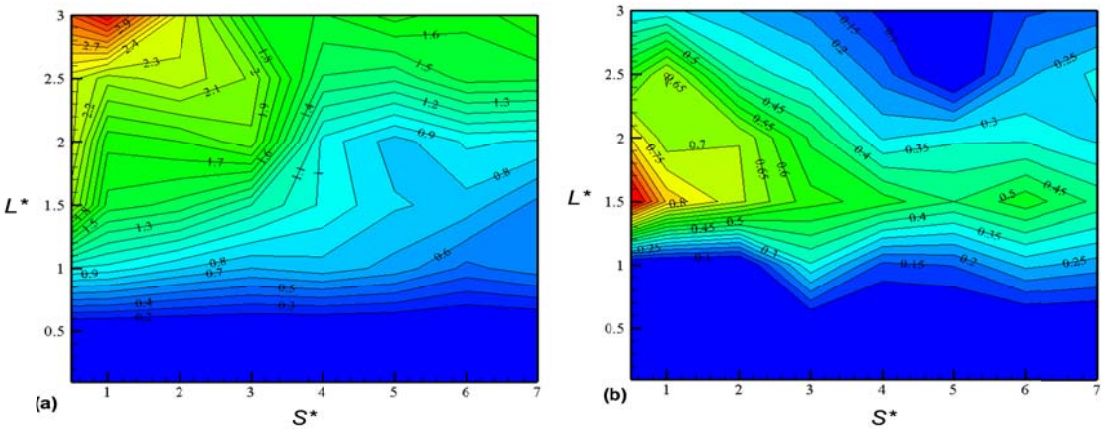

Fig. 8. Contours of RMS of lift coefficient of downstream cylinder (C_L') : (a) a*=1.0 and (b) a*=0.5 at different L* and S*.

5.3 Time averaged forces

To understand the effect of position and shape of the upstream cylinder on the forces of the downstream cylinder, contour diagram is presented for the normalized time averaged drag C_D and lift C_L coefficients for different a* at different L* in Fig.9 (C_D) and 10 (C_L). The averaged force coefficients are normalized with the corresponding single isolated cylinder values at Re=100. The C_D of the downstream cylinder for both a* shows qualitatively similar behavior with changing the gap height. Apparently, the variation of C_D with L* and a* is found maximum upto the intermediate gap spacing (S*= 3), and minimum for larger spacings (S* = 7). The mean drag coefficient decreases nominally up to gap height L* = 0.5, then increases very rapidly and crosses the value of a single isolated cylinder. This jump in C_D corresponds to a change in flow pattern, when the vortex shedding from the cylinder starts. As seen in Fig. 11, the negative gauge pressure is found to act on the rear face of the downstream cylinder and it increases with gap height. It results to increase in the formation of stronger vortices (ref. Fig. 4 and 5). For offsetting case near L* = 1.0, the C_D is very near to the isolated value for all a* and S*. A range of L* at which negligible drag force on the downstream cylinder can be noted from Fig. (9).

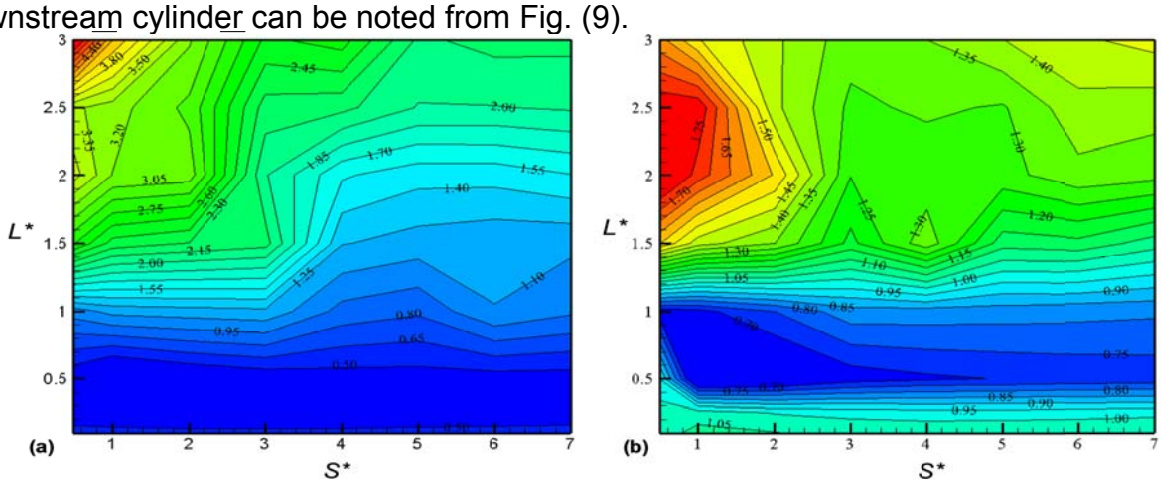

Fig. 9. Contours of normalized time averaged drag coefficient (C_D) of downstream cylinder : (a) a*=1.0 and (b) a*=0.5 at different L* and S*.

Similar to the C_D, the behavior of C_L coefficient with a* and L^* on the downstream cylinder is mostly same at respective spacing, for example, the effect is minimum at S^* = 7. However, the presence of the upstream cylinder has less effect on lift force on the downstream cylinder in comparison to its drag counterpart for all S^*. The maximum reduction in C_L of the downstream cylinder is found around L^* = 1 for all S^*, notably at S^* = 0.5. The downstream cylinder is found to be free from lift force for some higher values of L^*.

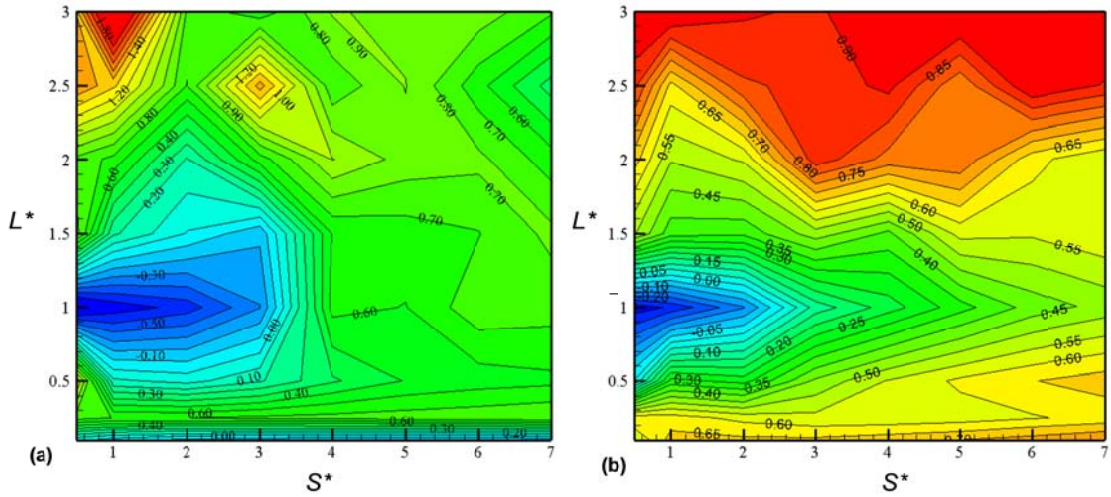

Fig. 10. Contours of normalized time averaged lift coefficient (C_L) of downstream cylinder : (a) a^*=1.0 and (b) a^*=0.5 at different L^* and S*.

The time-averaged surface pressure distribution $\overline{C}_P$ around the downstream square cylinder at selected values of L^* (considering three cases : closely spaced (S^* = 0.5), intermediate spacing (S* = 3.0), and large spacing (S*=7.0)) at various L^* is plotted in Fig. 11 (left side : a^* = 1.0 and right side : a^* = 0.5). The pressure is negative on the faces of the square cylinder with a suction ($-\overline{C}_P$) peak develop at the front of the undersurface. The $\overline{C}_P$ distribution on the downstream cylinder front face is strongly affected by the presence of the upstream cylinder, remarkably for a^* = 1.0. It is observed that variation in L^*, the distribution of $\overline{C}_P$ are biased towards the top leading edge. At lower $L^* \leq 0.25$, the $\overline{C}_P$ distribution is same for both a^*. Reduction of height results shift in the location of the maximum pressure on the front face. The difference in pressure distribution (between the front and rear faces of the cylinder) increases with the increase in L^*, indicating that the drag force increases with increase in L^*. Due to presence of the upstream cylinder, the pressure on the front face of the downstream cylinder is reduced from the isolated single cylinder value. While offsetting the upstream cylinder from inline arrangement and the wall the average pressure approaches to the isolated value. For a^* = 0.5, at large gap height the average pressure distribution on the downstream cylinder is similar and approaches to the single cylinder pressure distribution. It is noted from Fig. 11 that for a^* = 0.5 the effect of presence of the upstream cylinder is reduced compared to a^* = 1.0. The difference in pressure distribution for different a^* is associated with the variation in vortex formation length and strength of vortices behind the cylinder.

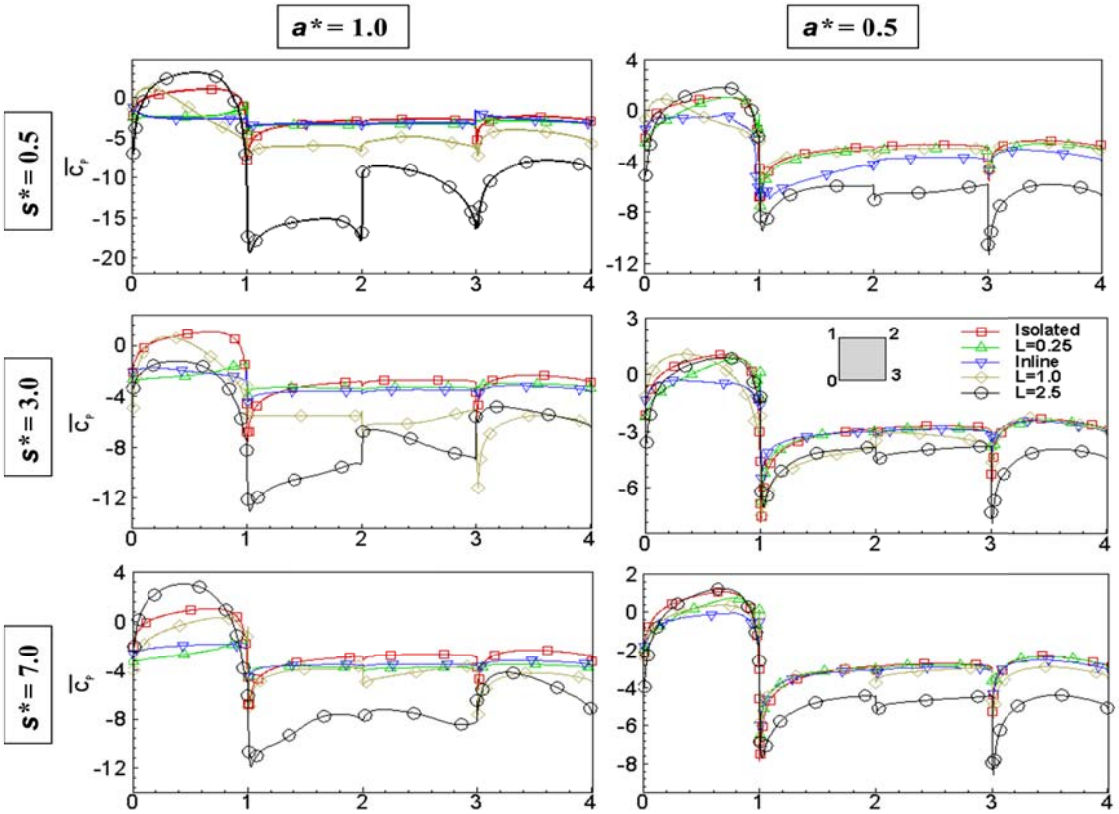

Fig. 11. Time-averaged surface pressure distribution around the downstream cylinder in absence and presence of upstream square cylinder of different *a** for different *L** and *S**.

6. CONCLUSIONS

This study presents the numerical investigation of flow around a square cylinder in presence of upstream square cylinder of different heights in staggered arrangement in proximity to a wall under the incidence of uniform shear flow. The following observations are reported from this study :

- The wake flow of the downstream square cylinder is significantly affected by the position (*L** and *S**) and height of the upstream square cylinder. For lower *L** flow remains steady similar to the single isolated cylinder, while increase in *L** results unsteady flow from the downstream square cylinder and it becomes complex at higher *L**. Reduction of height of upstream cylinder (*a** = 0.5) results reduction in the large stretched vortices into regular vortices.

- The pressure difference between the front and rear faces of the downstream cylinder increases with increase in the gap height (*L**) and it results to increase the average drag force on the downstream cylinder. The effect of *L*, a** on C_D is maximum at the intermediate spacing (*S** ≈ 3.0), while minimum at the large spacing (*S** ≈ 7.0). The C_D decreases for the inline tandem position (*L** = 0.5) then increases rapidly and crossed the isolated cylinder value as *L** increases. The

effect of size and position have negligible effect on the average forces of the downstream cylinder at large spacing.

- For closely spaced the intensity of peak of spectra decreases with increase in L^* for both the values of a^*. The shedding frequency increases with increase in L^* and this value is more for the case of a^*= 0.5. However, the C_{Lrms} value is more for a^* = 1.0. Beyond certain L^* these values either remain constant or decrease with increase in L^*. It is therefore noticed that at large L^* the presence of upstream cylinder is negligible.

ACKNOWLEDGMENTS

The authors acknowledge financial assistance of DST (INDIA) (San No. 100/IFD/3613/2008-09) and UGC-BSR (INDIA) (letter no.F.4-1/2006(BSR)/7-203/2009) for carrying out this work. Alam wishes to acknowledge the support given to them from National Natural Science Foundation of China through Grants 11672096 and from Research Grant Council of Shenzhen Government through grant JCYJ20160531191442288.

REFERENCES

Akbari, M.H. and Price, S.J., (2005), “Numerical investigation of flow patterns for staggered cylinder pairs in cross-flow”, *Journal of Fluids and Structures* **20**, 533–554.

Alam, M.M., Sakamoto, H., and Zhou, Y., (2005), “Determination of flow configurations and fluid forces acting on two staggered circular cylinders of equal diameter in cross-flow”, *Journal of Fluids and Structures* **21,** 363–394.

Alam, M.M., Zheng, Q., and Hourigan, K., (2017), “The wake and thrust by four side-by-side cylinders at a low Re”, *Journal of fluids and Structures*, **70**, 131-144.

Burattini, P., and Agrawal, A., (2013), “Wake interaction between two side-by-side square cylinders in channel flow”, *Computers and fluids*, **77**, 134–142.

Balachandar, S., and Parker, S.J., (2002), “Onset of vortex shedding in an inline and staggered array of rectangular cylinders”, *Physics of fluids* 1070-6631/2002/14(10)/3714/19/19.00.

Bhattacharyya, S. and Maiti, D.K. (2004), “Shear flow past a square cylinder near a wall”, *In. Journal of Engineering Science* **42**, 2119-2134.

Bhattacharyya, S., and Maiti, D.K., (2005), “Vortex shedding from a square cylinder in presence of a moving ground”, *Int. J. Numer. Meth. Fluids* **48**, 985-1000.

Bhattacharyya, S., Maiti D.K, and Dhinakaran S., (2006), “Influence of buoyancy on vortex shedding and heat transfer from a square cylinder in wall proximity”, *Numer heat transfer: Part A*, **50**, 585–606.

Bhattacharyya, S. and Dhinakaran, S. (2008), “Vortex shedding in shear flow past tandem square cylinders in the vicinity of a plane wall”, *Journal of Fluids and Structures* **24**, 400-417.

Bao, Y., Qier, W., and Zhou, D., (2012), “Numerical investigation of flow around

an inline square cylinder array with different spacing ratios", *Computers and Fluids*, **55,** 118–131.

Cheng, M., Tan, S.H., and Hung, K.C., (2005), "Linear shear flow over a square cylinder at low Reynolds number", *Phys. Fluids*, **17**, 078103.

Chatterjee, D., Biswas, G., and Amiroudine, S., (2010), "Numerical simulation of flow past row of square cylinders for various separation ratios", *Computers and fluids* **39**, 49–59.

Chern, M.J., Kanna, P.R., Lu, Y.J., Cheng, I.C. and Chang, S.C., (2010), "A CFD study of the interaction of oscillatory flows with a pair of side-by-side cylinders", *Journal of fluid and structures*, 626–643.

Davis, R.W. and Moore, E.F. (1982) "A numerical study of vortex shedding from rectangles", *J. Fluid Mech.* **116**, 475–506.

Devarakonda, R., (1994), "Experimental and numerical investigation of unsteady bluff body flows", Ph.D. Thesis, University of California at Berkeley, Berkeley, CA.

Franke, R., Rodi, W. and Schonung, B. (1990) "Numerical calculation of laminar vortex shedding flow past cylinders", *J. Wind Eng. Ind. Aerodyn.* **35**, 237–257.

Harichandan, A.B. and Roy, A., (2012), "Numerical investigation of flow past single and tandem cylindrical bodies in the vicinity of a plane wall", *Journal of Fluids and Structures* **33**, 19–43.

Lee, K. and Yang, K.S., (2009), "Flow patterns past two circular cylinders in proximity", *Computers & Fluids*, **38**, 778–788.

Leonard, B.P. (1995), "Order of accuracy of QUICK and related convection-diffusion Schemes", *Appl. Math. Model.* 19, 640–653.

Maiti, D.K. (2011), "Dependence of flow characteristics of rectangular cylinders near a wall on the incident velocity", *Acta Mechanica* **222**, 273–286.

Maiti, D.K. (2012), "Aerodynamic Characteristics of Rectangular Cylinders Near a Wall", *Ocean Engineering*, **54,** 251-260.

Malekzadeh, S., and Sohankar, A., (2012), "Reduction of fluid forces and heat transfer on a square cylinder in a laminar flow regime using a control plate", *Int J Heat Fluid Flow*, **34,** 15–27.

Maiti, D.K., Bhatt, R., (2014a), "Numerical study on flow and aerodynamic characteristics: Square cylinder and eddy-promoting rectangular cylinder in tandem near wall", *Aerospace Science Tech*., **36**, 5–20.

Maiti, D.K., and Bhatt, R., (2014b), "Vortex shedding suppression and aerodynamic characteristics of square cylinder due to offsetting of rectangular cylinders towards a plane", *Ocean Eng*., **82**, 91–104.

Martinuzzi, R.J., Bailey, S.C.C. and Kopp, G.A. (2003), "Influence of wall proximity on vortex shedding from a square cylinder", *Experiments in Fluids* **34**, 585–596.

Mahir, N., (2009), "Three-dimensional flow around a square cylinder near a wall", *Ocean engineering*, **36, 357-367.**

Niu, J. and Zhu, Z., (2006), "Numerical study of three-dimensional flows around two identical square cylinders in staggered arrangements", *Physics of fluid*, **18**, 044106.

Okajima, A. (1990) "Numerical simulation of flow around rectangular cylinder", *J.*

Wind Eng. Ind. Aerodyn. **33**, 171–180.

Patankar, S.V. (1980), “Numerical Heat Transfer and Fluid Flow”. Hemisphere Publishing Corporation, Taylor & Francis Group, New York.

Rosales, J.L., Ortega, A., and Humphrey, J.A.C., (2000), “A numerical investigation of convective heat transfer in unsteady laminar flow past a single and tandem pair of square cylinders in a channel”, *Numer Heat Transfer : Part A* **38**, 443–465.

Sewatkar, C.M., Sharma, A. and Agrawal, A., (2009), “On the effect of Reynolds number for flow around a row of square cylinders”, *Physics of fluids* **21**, 83602.

Saha, A.K., Muralidhar, K. and Biswas, G., (2003), “Investigation of two- and three-dimensional models of transitional flow past a square cylinder”, *Journal of Eng. Mechanics*, **129, 11.**

Sumner, D., Price, S.J. and Paidoussis, M.P., (2000), “Flow-pattern identification for two staggered circular cylinders in cross-flow”, *J. Fluid Mech*., **411**, 263-303.

Zhou, Y., Feng, S.X., Alam, M.M. and Bai, H.L., (2009), “Reynolds number effect on the wake of two staggered cylinders”, *Physics of fluids*, **21**, 125105.